Machine Vision and Applications (2012) 23:91–109
DOI 10.1007/s00138-010-0294-8

ORIGINAL PAPER

Network snakes: graph-based object delineation with active contour models

Matthias Butenuth · Christian Heipke

Received: 4 November 2009 / Revised: 7 July 2010 / Accepted: 8 August 2010 / Published online: 30 August 2010
© Springer-Verlag 2010

Abstract In this paper, a graph-based method of active contour models called network snakes is presented and investigated. Active contour models are a well-known method in computer vision, bridging the gap between low-level feature extraction or segmentation and high-level geometric representation of objects. But the original concept is limited to single closed object boundaries. Network snakes are the method enabling a free optimization of arbitrary graphs representing the geometric position of networks and boundaries between adjacent objects. The main impacts of network snakes are the combination of the image energy representing objects in the real world, the internal energy incorporating shape characteristics, and the topology representing the structure of the scene. The introduction and exploitation of the topology in a comprehensive energy functional turn out to be a powerful technique to cope with complex questions of object delineation from imagery. Network snakes are analyzed and evaluated with both synthetic and real data to point out the role of the required initialization, the benefit of the introduced topology and the transferability. Exemplary investigated real applications are the delineation of field boundaries from remotely sensed imagery, the refinement of road networks from airborne SAR images and bio-medical tasks delineating adjacent biological cells in microscopic images. Concluding remarks are given at the end to discuss potential future research.

M. Butenuth (✉)
Remote Sensing Technology, Technische Universität München, Munich, Germany
e-mail: matthias.butenuth@bv.tum.de

C. Heipke
Institute of Photogrammetry and GeoInformation, Leibniz Universität Hannover, Hannover, Germany

Keywords Active contour models · Networks · Graphs · Topology · Optimization

1 Introduction

Active contour models are a powerful, physics-based technique which is employed in various parts of computer vision and computer graphics, for instance, segmentation, reconstruction, registration, recognition, and manipulation of non-rigid curves or surfaces from images and image sequences. The so-called snakes were introduced as a first contribution to this research field with the seminal paper by [17]. The innovation of the method is to bridge the gap between low-level feature extraction or segmentation and high-level geometric representation of objects. The technique can also be regarded as a method to delineate subjective contours or surfaces [16], i.e. to derive good results even though the object of interest is only partly represented in the image. Active contour models have received a lot of attention in the last two decades, as reflected in numerous contributions, for an overview, see [1,27]. Different applications using active contour models have been investigated, for example, remote sensing applications [13,19,30], the tracking of objects in image sequences [8,28] and medical image applications [22,24,32,35].

1.1 State of the art

Two directions of active contour models have been developed as complements to each other: *parametric active contours* [17] and *geometric active contours* [5,23]. The main difference is the explicit representation of parametric active contours compared to the implicit representation of geometric

active contours. Parametric active contours allow for an easy direct interaction during the optimization while geometric active contours are parameterized after curve evolution and a direct interaction needs more efforts. On the other hand, the implicit representation enables topological changes during the evolution, whereas the topology of parametric active contours is rigid and splitting or merging is complicated. However, the idea behind both concepts is quite similar: the coupling of the image data with an internal energy in an energy minimization framework for parametric active contours or the combination of the level set method with the curve evolution theory concerning geometric active contours. Both models, parametric and geometric active contours, are originally defined for single closed object contours. For this reason, advanced research extended these models to facilitate solutions dealing with more than one object.

Contributions concerning *multiple parametric active contours* are addressed in [25] to handle multiple snakes with the additional opportunity to deal with topological changes. A domain decomposition framework is proposed with an iterative re-parameterization using a superimposed grid. The case of multiple 3D deformable models with automated topology changes is examined in [18], based on the work of [20], where a generic model is presented to recover multiple shapes or to extract multiple surfaces from 3D data. The approach of [9] detects intersections of edges controlling connected components automatically to eliminate overlaps of object contours. In the work of [31], several contours are initialized and evolve separately with the aim to merge those within homogeneous image regions.

Research regarding *multiple geometric active contours* is also discussed in several contributions. In the work of [44], the authors use as many level set functions as the expected kinds of regions. Depending on the proximity, each level set moves to the nearest interface, overlaps and gaps are removed in a separate reassignment step. Similarly, the exploitation of prior knowledge concerning the number of regions characterized by a predetermined set of statistical features is the starting point of the work presented in [42]. Geodesic active regions are utilized in [29] to deal with frame partition problems. The authors integrate boundary and region-based information within a curve-based minimization framework incorporating expected properties of defined classes. A multiphase level set formulation is given in [6,37] to avoid the construction problems of overlaps and gaps during image segmentation. However, the used region information to define the boundaries of the segments is only reasonable for the delineation of particular object classes.

The discussed work above concerning multiple active contours does not cover the general problem of adjacent or partly touching objects, where a change of topology is not desired. *Coupled active contours* incorporate topological constraints to cope with similar image energies characterizing neighboring objects. Regarding *coupled parametric active contours*, one example is the work of [47]: the authors include a penalty force during the simultaneous optimization of all contours taking into account that objects cannot merge during the optimization. Thus, tasks such as tracking of objects represented with similar intensities or textures are possible without losing the given topology under the assumption of a homogeneous background. Work related to *coupled geometric active contours* is more common, first discussed in [26]. The authors enhance the traditional level set formulation, implying only one interface separating two regions, to a coupled level set method dealing with multiple level sets having multiple junctions. The difficulty lies in establishing a constraint at triple junctions that couples the three functions at a single point. In the cited approach, this is achieved at each time step with a kind of interface operation. This point is solved in the contribution of [33] by replacing each level set function after the movement with a correction term defined by the overlap of neighbored level sets. The handling of multiple objects with multiple level sets is addressed in [43], where a coupling constraint minimizes the overlap of touching objects. However, it is not guaranteed that the boundary between touching objects is correctly located. Topological constraints are introduced in the contribution of [14] to preserve the given initial topology. The simple point criterion from digital topology is applied by evaluating the implicit contour during the evolution to avoid overlapping segments. A further article dealing with the preservation of topology is given in [36] in form of a polygon regularizer, particularly suitable for textured objects. The approach prevents topology changes, but adjacent polygons can still touch. In the work of [34], the authors propose an enhancement by gradually adjusting the original flow and a global regularization scheme to avoid geometrical inaccuracies when preserving the topology. Again, the given initial topology is identified as an important prior knowledge to be considered during curve evolution.

The mentioned approaches of multiple and coupled active contours require particular conditions to handle multiple objects such as homogeneous object representations in terms of intensities, colors or statistical properties, which are only suitable for specific segmentation applications. Alternatively, additional steps of re-parameterizations of the contour are needed during the optimization. The general question on how to represent multiple and adjacent objects with only *one* boundary in-between is unanswered. Moreover, the delineation of adjacent objects without any available homogeneous object characteristics within the segments is unsolved. In addition, objects represented directly by *networks* independently of object and, thus, purposive image information of the enclosed network segments, are not covered by the discussed approaches.

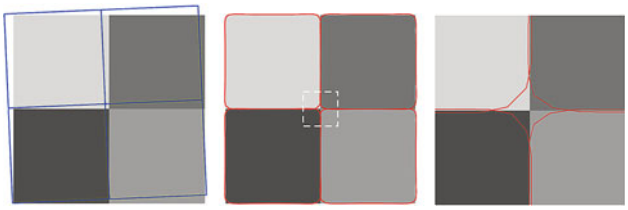

Fig. 1 Delineating adjacent objects with traditional parametric active contours: initialization (*blue*), result and zoomed result part (*red*)

1.2 Graph-based optimization with active contour models

The main goal of this paper is the development of a new method of active contour models that enable the optimization of an arbitrary *graph* representing the geometric image space positions of *networks* and *boundaries between adjacent objects*. The discussion of the state of the art points out the need to deepen the understanding concerning the delineation of adjacent objects, which are separated by only a single boundary, and to develop solutions which enable the delineation of networks. A new graph-based method of active contour models called *network snakes* with a well-defined mathematical model is proposed in this paper.

In Fig. 1, a synthetic example is taken to demonstrate the general limitation of the traditional concept of parametric active contours and to identify the challenge of this paper. The four regions cannot be delineated with one contour jointly; instead for each segment a single and closed contour is required. Starting from a topologically correct initialization (Fig. 1, left), the optimization leads to changes in topology and thus to incorrect results (Fig. 1, middle). Focusing on the center of the synthetic example (dashed white line), the gaps and overlaps of the result are more apparent (Fig. 1, right). This consequence is mathematically obvious, because the individual contours do not consider adjacent ones due to the fact that no topological knowledge about the objects of interest is incorporated in the model of parametric active contours.

Three sub-goals can be defined as follows:

- Development of a new method of active contour models which optimizes the geometric position of graphs consisting of nodes of an arbitrary degree to enable the delineation of open contours, closed contours and networks.
- Development of a new method of active contour models which segments imagery without gaps or overlaps to enable the delineation of adjacent objects and networks.
- Development of a new method of image segmentation and object delineation with a high generality and transferability to enable its applicability for a variety of tasks.

The term network snakes was already used in the work of [11,12]. The authors insert a local network to reconstruct 3D-buildings: trihedral corners impose constraints of 90° angles between the three edges terminating at the corners. Thus, the approach is only suitable for particularly constrained applications and a free movement of all nodes and edges during the optimization is not possible. In contrast, the goal of this paper is to develop a general and comprehensive method enabling a free movement of all nodes and edges of a graph during the optimization without any particular constraints. Partly related work to the stated goals are adaptive adjacency graphs as introduced in [15] and enhanced in [10] to extract networks of active contours. The authors connect active contours at nodes during the deformation. The connectivity of the graph is achieved by imposing external energies in the form of constraints or springs to keep the adjacent contours together. However, a mathematical basis of the nodes with a degree unequal to two is not given and holes can appear leading to an incorrect topology. This fact contradicts to the aims of this paper in terms of a well-defined mathematical model including a correct topology. A further related framework concerning the defined goals is the region competition approach for image segmentation presented in [45,46] combining active contours and region growing techniques to minimize a global cost function. The used generalized minimum description length (MDL) criterion assumes regions with smooth boundaries and homogeneous intensity properties within the image, which are defined by a list of probability distributions. A topological control of adjacent objects is not incorporated into the proposed approach. Similarly, a global minimization of active contours is proposed in [2] to avoid the dependence of the initial guess of the contour. The authors introduce an edge indicator function to improve the solely region-dependent image energy. But again, a topological control is not included why only partly represented object boundaries in the image are hardly detectable.

The development of a general method satisfying the goals of this paper has so far not been obtained, which not only points out the methodical contribution, but also emphasizes the impact to different real application scenarios. Potential applications are for instance the delineation of road networks or field boundaries from remotely sensed imagery, bio-medical tasks such as the delineation of adjacent biological cells in microscopy cell imagery or industrial applications. A further goal of this paper is to develop a new method of active contour models with a high generality and transferability concerning the delineation of adjacent objects and any networks. The aim is to enable a free optimization of the whole network considering a complete control of the object shape at any contour parts. The incorporation of geometric constraints and, thus, the limitation of the method to only particular applications is not desired.

One important criterion is the possibility to control and exploit the *topology*, particularly when dealing with applications based on noisy image data or weak object

representations. This criterion points to parametric active contours for further investigations due to their explicit representation of the contours. Even though a given topology is required or has to be derived from the initialization, the large benefit is the *joint* exploitation of the traditional energy terms of active contours together with the newly introduced topology represented in a graph. Thus, poor object representations in imagery can still enable good object delineations supported by the proposed graph-based optimization. A second important factor is the underlying image energy: geometric active contours incorporate methodically the whole image domain, even though approaches often use only a narrow band around the contour to speed up processing. Parametric active contours use local image information during the optimization, which is a disadvantage when the object topology is unknown, but an advantage when the topology is known or no (region-based) image information is available to specify topological changes. In particular, if the required image information is only given at adjacent segment borders or just at the geometric image space positions of the network itself, the explicit concept is advantageous.

First ideas and concepts regarding network snakes are presented in the work of [3,4]. However, the contribution of [4] only contains the idea that parametric active contours should be enhanced to deal with networks not including a mathematical model of network snakes. The paper of [3] introduces a draft mathematical concept, but not the complete framework which is required to deal with arbitrary networks of active contours. In contrast, this paper defines the general model of network snakes and the required implementation issues. For the first time, systematic investigations regarding the initialization conditions, the benefit of the exploitation of the topology and the generality are achieved using synthetic examples. In addition, the method is applied to three different real application scenarios to demonstrate the transferability including an evaluation with numerical values. Thus, this paper presents for the first time the overall approach including its potential and limitations.

The next section presents the details of the mathematical basis and the energy minimization concept of parametric active contours. In Sect. 3, the new method of network snakes is presented. In Sect. 4, the developed method is analyzed and evaluated with both, synthetic and real data to point out its generality and transferability. Finally, in Sect. 5, concluding remarks are given to point out further investigations.

2 Basics

The state of the art and the defined goals result in a solution based on the concept of parametric active contours to develop the new method of network snakes. This section presents the basics and the details of the energy minimization concept to provide a mathematical basis for the proposed new method. We have introduced this section into the paper to make our contribution more self-contained. Readers familiar with parametric active contours and the related energy minimization scheme may wish to skip this section and continue directly at Sect. 3.

2.1 Parametric active contours

A traditional parametric active contour, often called a *snake*, is defined as a parametric curve C

$$C(s) = (x(s), y(s)), \tag{1}$$

where $s \in [0,1]$ is the arc length, and x and y are the coordinates of a closed 2D-curve. The core of active contour models is to let the curve C evolve in an image I delineating the object of interest. This aim is reached by minimizing an appropriate energy functional $E(C(s))$ [17]:

$$\begin{aligned} E(C(s)) &= \int_0^1 E_{\text{curve}}(C(s))\,\mathrm{d}s \\ &= \int_0^1 \left[E_{\text{img}}(C(s)) \right. \\ &\quad \left. + E_{\text{int}}(C(s)) + E_{\text{con}}(C(s))\right]\mathrm{d}s \\ E(C(s)) &\rightarrow \min. \end{aligned} \tag{2}$$

The energy functional consists of the *image energy* $E_{\text{img}}(C(s))$ representing an optimal description of the object of interest in the image, the *internal energy* $E_{\text{int}}(C(s))$ introducing modeled object knowledge concerning the shape and movement behavior of the object and, finally, the *constraint energy* $E_{\text{con}}(C(s))$ offering the possibility to insert any external constraints to the energy functional. The constraint energy $E_{\text{con}}(C(s))$, can e.g. be used to fix a point at a predefined position. $E_{\text{con}}(C(s))$ is an optional part of the snakes concept, however, and not further considered here (see the topology preserving energy term discussion in Sect. 3.2 below). The minimization of the energy functional $E(C(s))$ is accomplished using an iterative scheme starting from a given initialization.

The image energy $E_{\text{img}}(C(s))$ describes the object of interest in the image I in an optimal manner, i.e. to let the contour C being attracted by salient features in the image representing the boundaries of the object of interest. In the simplest way, the image energy can be expressed by the image intensities themselves with

$$E_{\text{img}_{\text{line}}}(C(s)) = I(C(s)) \tag{3}$$

to detect light or dark lines. When the object of interest is characterized by edges, the image energy can be defined as

$$E_{\text{img}_{\text{edge}}}(C(s)) = -|\nabla I(C(s))|^2, \tag{4}$$

where $|\nabla I(C(s))|$ is the norm or magnitude of the gradient image at the coordinates $x(s)$ and $y(s)$. The negative sign results in an attraction of the contour to large image gradients during energy minimization. An alternative image energy that significantly increases the capture range while preserving accurate image boundaries is the distance potential force introduced by [7]. A distance map $d(x, y)$ is derived by calculating the distance between each pixel and the closest already extracted edge point. An appropriate potential energy $P_{\text{dist}}(C(s))$ can be defined as $P_{\text{dist}}(C(s)) = -\mathrm{e}^{-d(C(s))^2}$, and the corresponding image energy is given by

$$E_{\text{img}_{\text{dist}}}(C(s)) = -|\nabla P_{\text{dist}}(C(s))|. \tag{5}$$

A further image energy improving the distance map is the gradient vector flow (GVF), which aims at overcoming the general problem of concave boundary regions [40,41]. It might be helpful to utilize more than one resolution when minimizing the energy functional of active contour models, examples for the combination of different resolutions are given in [21,39].

The second term of the energy functional representing the active contour model is the internal energy $E_{\text{int}}(C(s))$. The aim is to incorporate prior knowledge about the shape characteristics or movement of the object of interest during the energy minimization. The internal energy $E_{\text{int}}(C(s))$ is defined as

$$E_{\text{int}}(C(s)) = \frac{1}{2}\left(\alpha(s)\cdot|C_s(s)|^2 + \beta(s)\cdot|C_{ss}(s)|^2\right), \tag{6}$$

where C_s and C_{ss} are the first and second derivatives of C with respect to s [17]. The first term of the internal energy, weighted by $\alpha(s)$, controls the elasticity or tension of the curve. Large values of $\alpha(s)$ allow the contour to become very straight between two points and hamper stretching, while small values allow a higher bending. The second term of the internal energy, weighted by $\beta(s)$, controls the rigidity of the curve. Large values of $\beta(s)$ let the contour become smooth, and small values allow the generation of corners.

2.2 Energy minimization

In this section, the minimization of the energy functional $E(C(s))$ of parametric active contours is given in detail. In general, the calculus of variations deals with seeking a curve (or surface), for which a given functional $F(C)$ in the form of

$$F(C) = \int_0^1 E(s, C, C_s, C_{ss})\,\mathrm{d}s \tag{7}$$

has a minimum or maximum considering the boundary conditions $C(0) = C_b, C(1) = C_e$, where the values $C_e > C_b$ are given, and with $C_s = \partial C/\partial s$, $C_{ss} = \partial^2 C/\partial s^2$. The solution of the functional $F(C)$ defined in (7) is obtained by setting up the condition $C(s) = C_0(s) + \varepsilon\eta(s)$, where $\eta(s)$ is a function with $\eta(0) + \eta(1) + \eta_s(0) + \eta_s(1) = 0$. Using the above definition, the functional $F(C)$ is replaced with the function $F(\varepsilon)$, i.e. the variational problem becomes an extremum problem

$$F(\varepsilon) = \int_0^1 E\left(s, C_0 + \varepsilon\eta,\ C_{0_s} + \varepsilon\eta_s,\ C_{0_{ss}} + \varepsilon\eta_{ss}\right)\mathrm{d}s, \tag{8}$$

fulfilling the condition $\partial F/\partial\varepsilon = 0$ for $\varepsilon = 0$. Using the Taylor expansion one gets

$$\begin{aligned} F(\varepsilon) &= \int_0^1 \Bigg(E(s, C_0, C_{0s}, C_{0ss}) + \frac{\partial E}{\partial C}(s, C_0, C_{0s}, C_{0ss})\,\varepsilon\eta \\ &\quad + \frac{\partial E}{\partial C_s}(s, C_0, C_{0s}, C_{0ss})\,\varepsilon\eta_s \\ &\quad + \frac{\partial E}{\partial C_{ss}}(s, C_0, C_{0s}, C_{0ss})\,\varepsilon\eta_{ss}\Bigg)\mathrm{d}s. \end{aligned} \tag{9}$$

The introduced condition defined above leads to

$$\begin{aligned} &\int_0^1 \eta\left(\frac{\partial E}{\partial C}\right)\mathrm{d}s + \int_0^1 \eta_s\left(\frac{\partial E}{\partial C_s}\right)\mathrm{d}s \\ &\quad + \int_0^1 \eta_{ss}\left(\frac{\partial E}{\partial C_{ss}}\right)\mathrm{d}s = 0, \end{aligned} \tag{10}$$

and with integration by parts considering the boundary conditions for $\eta(s)$ it follows

$$\int_0^1 \eta\left(\frac{\partial E}{\partial C} - \frac{d}{\mathrm{d}s}\left(\frac{\partial E}{\partial C_s}\right) + \frac{d^2}{\mathrm{d}s^2}\left(\frac{\partial E}{\partial C_{ss}}\right)\right)\mathrm{d}s = 0. \tag{11}$$

The integral of (11) vanishes for every function $\eta(s)$ resulting in

$$\frac{\partial E}{\partial C} - \frac{d}{\mathrm{d}s}\left(\frac{\partial E}{\partial C_s}\right) + \frac{d^2}{\mathrm{d}s^2}\left(\frac{\partial E}{\partial C_{ss}}\right) = 0 \tag{12}$$

which represents the general Euler differential equation.

In the following, this general solution is applied to the minimization of the energy functional $E(C(s))$ of parametric active contours. With constant weight parameters $\alpha(s) = \alpha$ and $\beta(s) = \beta$ in order to simplify the representation, the energy functional $E(C(s))$ of parametric active contours given in (2) can be minimized by solving the corresponding Euler equations:

$$\frac{\partial E_{\text{img}}}{\partial C} - \alpha \frac{\partial^2 C}{\partial s^2} + \beta \frac{\partial^4 C}{\partial s^4} = 0. \tag{13}$$

As the contour C is represented with the coordinates x and y, cf. (1), (13) results in two independent equations concerning both coordinates. The derivatives are approximated with finite differences since they cannot be computed analytically:

$$\begin{aligned} &\frac{\partial E_{\text{img}}}{\partial C} + \alpha \left((C_i - C_{i-1}) - (C_{i+1} - C_i) \right) \\ &+ \beta \left(C_{i-2} - 2C_{i-1} + C_i \right) - 2\beta \left(C_{i-1} - 2C_i + C_{i+1} \right) \\ &+ \beta \left(C_i - 2C_{i+1} + C_{i+2} \right) = 0. \end{aligned} \tag{14}$$

With $\partial E_{\text{img}} / \partial C = f_C(C)$ (14) can be rewritten in matrix form as

$$AC + f_C(C) = 0. \tag{15}$$

A is a pentadiagonal band matrix of dimension n, which depends only on the parameters α and β. With substitution of $a = \beta$, $b = -\alpha - 4\beta$ and $c = 1 + 2\alpha + 6\beta$ the matrix A has the following structure for a closed contour:

$$A = \begin{bmatrix} c & b & a & 0 & \dots & 0 & a & b \\ b & c & b & a & 0 & \dots & 0 & a \\ a & b & c & b & a & 0 & \dots & 0 \\ 0 & a & b & c & b & a & \ddots & \vdots \\ \vdots & \ddots & \ddots & \ddots & \ddots & \ddots & \ddots & 0 \\ 0 & \dots & 0 & a & b & c & b & a \\ a & 0 & \dots & 0 & a & b & c & b \\ b & a & 0 & \dots & 0 & a & b & c \end{bmatrix}. \tag{16}$$

In general, the calculus of variations defines boundary conditions, which for parametric active contours are incorporated by fixed boundary values. For closed contours, the condition that the first point is identical to the last one is introduced, leading to additional entries in the upper right and the lower left corner of the matrix A.

A solution to (15) can be derived by setting the right hand equal to the product of a step size γ and the negative time derivatives of the left hand side. It is assumed that the derivatives of the image energy $f_C(C)$ are constant during the time step, i.e. $f_C(C_t) \approx f_C(C_{t-1})$, resulting in an explicit Euler step regarding the image energy. In contrast, the internal energy is an implicit Euler step due to its specification by the band matrix A. The resulting equation reads

$$AC_t + f_C(C_{t-1}) = -\gamma (C_t - C_{t-1}). \tag{17}$$

The time derivatives vanish at the equilibrium ending up in (15). Finally, a solution can be derived by matrix inversion:

$$C_t = (A + \gamma \mathrm{I})^{-1} (\gamma C_{t-1} - \kappa f_C(C_{t-1})), \tag{18}$$

where I is the identity matrix and κ is an additional parameter in order to control the weight between internal and image energy.

In the presented energy minimization process, two assumptions have been made. First, the approximation of the derivatives with finite differences (14) requires unit distances between neighboring points representing the contour. This prerequisite is important because parameterization changes can involve unwanted shape modifications [9]. In addition, the approximated curvature of the contour using finite differences will result in somewhat incorrect terms. Second, the parameter s is assumed to be the arc length to represent the curvature with the derivatives correctly [38]. In order to avoid re-parameterizations during the minimization process, a preservation of unit distances between neighboring points can be incorporated in the energy functional.

3 Network snakes

The presentation of the mathematical basics of parametric active contours and the discussion of the state of the art demonstrate that the goals of this paper cannot be reached with existing active contour models or related methodologies. To overcome this limitation, the new method of network snakes is introduced in this section.

3.1 Energy terms of network snakes

The new method of active contour models is represented by a *graph* to incorporate the topological characteristics of a contour network. The topology of the contour within the graph is defined by the nodes, which are characterized by the *degree of nodes* $\rho(C)$. An example is shown in Fig. 2: nodes with a degree $\rho(C) = 1$ represent *end points* of a contour, nodes with a degree $\rho(C) = 2$ represent a normal part of a contour and nodes with a degree $\rho(C) > 2$ represent nodes in which more than two edges terminate. In this work, the contour network is represented by a planar graph, i.e. it can be drawn in a plane without crossing graph edges. Having the possibility to distinguish between different *contour parts*, particularly when forming a network, each part of the whole contour is indexed as $C_A, C_B, \dots, C_Z$ (cf. Fig. 2). The nodes with a degree $\rho(C) \neq 2$ define the start or end points of the contour parts.

The crucial point concerning the introduction of the topology is the *internal energy* $E_{\text{int}}(C(s))$ of the energy functional representing the shape model (cf. Sect. 2). Regarding the minimization of the energy functional as defined in (7)–(18), a solution of the required Euler equations optimizing the internal energy $E_{\text{int}}(C(s))$ is only given for the traditional concept of parametric active contours. The reason is the approximation of the required derivatives with finite

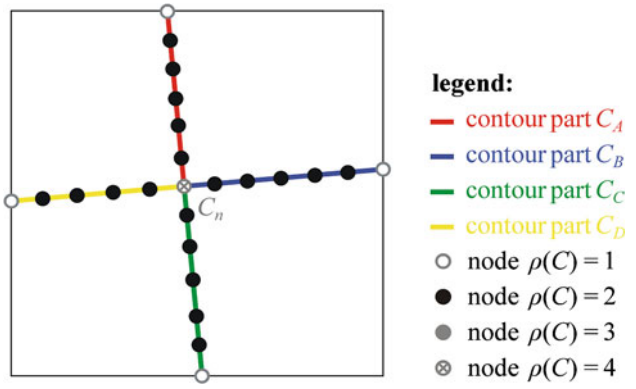

Fig. 2 Topology for network snakes

differences (14). The consequence of this prerequisite is that each node of the graph needs two neighboring nodes on both sides to compute the derivatives. Obviously, this condition is only fulfilled for closed object contours solely composed of nodes with a degree $\rho(C) = 2$ with an identical first and end point of the contour, i.e.$C_0 = C_n$. But, the utilized derivatives are not defined in the vicinity of nodes with a degree $\rho(C) \neq 2$, because the neighboring nodes are either not available at open contour ends (nodes with degree $\rho(C) = 1$) or exist multiple times (nodes with degree $\rho(C) > 2$), cf. the center of Fig. 2 for a node with a degree of $\rho(C) = 4$. Thus, the influence of the topology on the energy minimization of parametric active contours requires a new definition of the internal energy $E_{\text{int}}(C(s))$ to enable a shape control at every contour part.

The derivatives as defined above are not usable in the common way at nodes with a degree of $\rho(C) \neq 2$. In this work, the boundaries of adjacent objects are defined by *single contour parts* each ending in *single nodes*, where several contour parts are connected to each other. Obviously, the same definition is valid for the minimization of networks.

The proposed solution divides the given initial graph into separate contour parts $C_A, \ldots, C_Z$ connected at nodes C_n. In Fig. 2, a synthetic example is taken to exemplify the contour parts of the required network: the four contour parts C_A, C_B, C_C and C_D describe a part of a contour network representing for example the boundaries between adjacent objects, each of them is depicted with a separate color. In general, the contour parts meet with their respective end points $C_{A_n}, \ldots, C_{Z_n}$ in the common nodes C_n in such a way, that the end points of the contour parts define an identical point, i.e. $C_n = C_{A_n} = C_{B_n} = \cdots = C_{Z_n}$. Thus, the node C_n is contained in each connected contour part and, additionally, its position depends on the specific shape model of each contour part.

The *first term* of the internal energy (cf. (6)), weighted by the parameter α, cannot support the control of the internal energy in the vicinity of C_n during the energy minimization. The finite differences of the first term approximating the required derivatives are only uniquely available for the two nodes C_{n-1} and C_n but not for C_{n+1}. Thus, no shape control is possible and the first term is not considered during the energy minimization in the vicinity of nodes with a degree of $\rho(C) \neq 2$.

The *second term* of the internal energy, weighted by the parameter β, can partly aid the control of the shape behavior in the vicinity of C_n. This second term is rewritten using the available finite differences for the nodes C_{n-2}, C_{n-1} and C_n of each contour part separately to control the curvature of the contour network at nodes with a degree of $\rho(C) \neq 2$. The nodes C_{n+1} and C_{n+2} cannot support the calculation of the internal energy near C_n, because as before these nodes exist multiple times or do not exists. Thus, the internal energy has to be rewritten in the vicinity of the nodes C_n using the available finite differences for the nodes C_{n-2}, C_{n-1} and C_n . The new definition of the internal energy aims at controlling the shape of each contour part separately concerning its specific curvature up to each node C_n with degrees $\rho(C) \neq 2$ contained in the contour network. Simultaneously, the connectivity of the terminating contours at the nodes C_n has to be ensured. The new total energy functional for network snakes at the common nodes with a degree $\rho(C) \neq 2$ with $C_n = C_{A_n} = C_{B_n} = \cdots = C_{Z_n}$ is defined as

$$\begin{aligned}
&\beta\left(C_{A_n} - C_{A_{n-1}}\right) - \beta\left(C_{A_{n-1}} - C_{A_{n-2}}\right) + f_{C_A}(C_A) = 0\\
&\beta\left(C_{B_n} - C_{B_{n-1}}\right) - \beta\left(C_{B_{n-1}} - C_{B_{n-2}}\right) + f_{C_B}(C_B) = 0\\
&\beta\left(C_{C_n} - C_{C_{n-1}}\right) - \beta\left(C_{C_{n-1}} - C_{C_{n-2}}\right) + f_{C_C}(C_C) = 0\\
&\qquad\qquad\vdots\\
&\beta\left(C_{Z_n} - C_{Z_{n-1}}\right) - \beta\left(C_{Z_{n-1}} - C_{Z_{n-2}}\right) + f_{C_Z}(C_Z) = 0.
\end{aligned} \tag{19}$$

Each possible contour part $C_A, \ldots, C_Z$ terminating in one common node C_n is represented by one line in (19). The terms on the left side represent the new internal energy, the other terms $f_{C_A}(C_A), \ldots, f_{C_Z}(C_Z)$ represent the image energy at the respective contour parts. All contour parts $C_A, \ldots, C_Z$ intersect in the common single node C_n and can be optimized *simultaneously* when minimizing the energy functional of network snakes. The energy definition of (19) allows for an energy minimization controlling the shape of each contour part *separately* up to the common nodes C_n. At the same time, the exploitation of topology is ensured during the energy minimization process due to the connectivity.

The new definition of the internal energy in the vicinity of nodes with a degree $\rho(C) > 2$ introduced in (19) is similar to the part of the traditionally defined internal energy weighted by the parameter α, shown in (14). But, the parameter weighting the new internal energy is chosen to be β, because compared to α, it controls the shape behavior of the contours more naturally in terms of curvature and rigidity (cf. Sect. 2).

The new energy functional for network snakes developed above and defined in (19) is given exemplarily for a node with a degree $\rho(C) = 3$:

$$\frac{\partial E_{\text{img}}}{\partial C} + \beta \left(C_{A_{n-2}} + C_{B_{n-2}} + C_{C_{n-2}}\right) - 2\beta \left(C_{A_{n-1}} + C_{B_{n-1}} + C_{C_{n-1}}\right) + 3\beta \left(C_n\right) = 0. \tag{20}$$

The given energy functional of a node with a degree $\rho(C) = 3$ contained in (20) can be extended in a straightforward manner to nodes with higher degree. The general form can be written in matrix form as

$$A_n C + f_C(C) = 0. \tag{21}$$

image incorporating the given topology. Each contour part is assumed to consist of six nodes $C_0, \ldots, C_5$. The substitution for the energy minimization of network snakes is used with $a = \beta$, $b = -\alpha - 4\beta$, $c = 1 + 2\alpha + 6\beta$, $e = 1 + \alpha + 5\beta$, $f = -2\beta$ and $g = 1 + 4\beta$ to define the complete matrix A_n of the synthetic example. The matrix elements enclosed by the two dashed lines represents the node C_n with a degree $\rho(C) = 4$ connecting the four contour parts $C_A, \ldots, C_D$, the dotted lines mark the beginning and end of the respective contour parts. The new non-zero matrix elements besides the banded structure express the connecting parts representing the topology within the matrix A_n:

$$A_n = \begin{bmatrix}
a & f & a & 0 & \ldots & & & & & & & & & & & & & & & \\
f & e & b & a & 0 & \ldots & & & & & & & & & & & & & & \\
a & b & c & b & a & 0 & \ldots & & & & & & & & & & & & & \\
0 & a & b & c & b & a & 0 & \ldots & & & & 0 & 0 & & & & 0 & 0 & & \\
\ldots & 0 & a & b & e & f & 0 & 0 & \ldots & & 0 & f & a & 0 & & 0 & f & a & 0 & \\
\hdashline
 & \ldots & 0 & a & f & g & f & a & 0 & \ldots & & 0 & 0 & & & & 0 & 0 & & \\
\hdashline
 & & \ldots & 0 & 0 & f & e & b & a & 0 & \ldots & & & & & & & & & \\
 & & & \ldots & 0 & a & b & c & b & a & 0 & \ldots & & & & & & & & \\
 & & & & \ldots & 0 & a & b & c & b & a & 0 & \ldots & & & & & & & \\
 & & & & & \ldots & 0 & a & b & e & f & 0 & 0 & \ldots & & & & & & \\
 & & & & 0 & & \ldots & 0 & a & f & a & 0 & 0 & 0 & \ldots & & & & & \\
\cdots\cdots & & & & & & & & & & & & & & & & & & & \\
 & & & 0 & f & 0 & & \ldots & 0 & 0 & 0 & e & b & a & 0 & \ldots & & & & \\
 & & & 0 & a & 0 & & & \ldots & 0 & 0 & b & c & b & a & 0 & \ldots & & & \\
 & & & & 0 & & & & & \ldots & 0 & a & b & c & b & a & 0 & \ldots & & \\
 & & & & & & & & & & \ldots & 0 & a & b & e & f & 0 & 0 & \ldots & \\
 & & & & 0 & & & & & & & \ldots & 0 & a & f & a & 0 & 0 & 0 & \ldots \\
\cdots\cdots & & & & & & & & & & & & & & & & & & & \\
 & & & 0 & f & 0 & & & & & & & \ldots & 0 & 0 & 0 & e & b & a & 0 & \ldots \\
 & & & 0 & a & 0 & & & & & & & & \ldots & 0 & 0 & b & c & b & a & 0 \\
 & & & & 0 & & & & & & & & & & \ldots & 0 & a & b & c & b & a \\
 & & & & & & & & & & & & & & & \ldots & 0 & a & b & e & f \\
 & & & & & & & & & & & & & & & & \ldots & 0 & a & f & a
\end{bmatrix} \tag{22}$$

Now, the matrix A_n incorporates not only the parameters α and β controlling the shape, but also the given topology of the contour network. The matrix A of (15), (16) is adapted accordingly at the nodes with a degree $\rho(C) \neq 2$ and their neighbors to fulfill the new definition of the internal energy: some parts of the originally banded structure of the matrix are omitted to divide the contour parts, and other parts of the matrix are filled up to include the topology building further connections between different parts of the contour resulting in the desired network snakes.

One exemplary matrix A_n representing the topology of the synthetic example shown in Fig. 2, is given in (22) to demonstrate the structure of the new matrix A_n. The four contour parts $C_A, \ldots, C_D$ are connected at the common node C_n with a degree $\rho(C) = 4$ describing the objects of interest in the

Moreover, the elements of the matrix A_n missing in comparison to matrix A from (16) point out that there is no connection of the contour ends concerning their specific shape. The only link is given in the single node C_n representing the topology of the four contours within the network. Each contour part $C_A, \ldots, C_D$ is connected to the common node C_n on one end, and has an open contour end on the opposite side.

For this specific example, the open endings of the four contour parts are allowed to move only along the borderline, i.e. the x or y coordinate is fixed, respectively. In general, open end points can be controlled by introducing a length constraint to avoid a shrinking of the endings or, alternatively, a small variable length can be allowed based on image properties. The energy minimization of the synthetic example using network snakes is depicted in Fig. 3 to demonstrate the

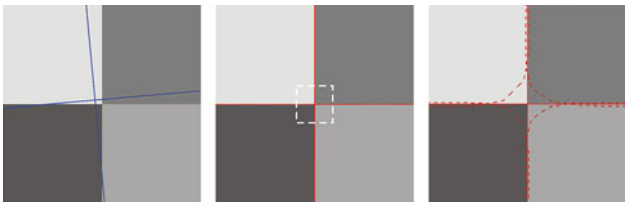

Fig. 3 Delineating adjacent objects with network snakes: initialization (*blue*), result and zoomed result part (*red*); dashed contour part (*dark red*) as comparison to traditional parametric active contours (cf. Fig. 1)

general functionality: starting from the initialization (Fig. 3, left), the contour moves step by step to the desired result (Fig. 3, middle). The given initial topology is preserved during the energy minimization process and, moreover, is also exploited. For example, the contour part C_A (top) is not close to the desired object boundary at the beginning, but as a result of the connection of the contour part to the network the contour part C_A is pulled to the correct object boundary. Focusing on the center of the synthetic example (dashed white line), no gaps or overlaps arise. Compared to the result of traditional parametric active contours (Fig. 1), the new method of network snakes by definition preserves the topology during the optimization leading to a correct result (Fig. 3, middle) and zoomed result part (Fig. 3, right).

3.2 Implementation

The implementation of the system is accomplished in an object-based computer language. Three general tasks are regarded here which must be considered realizing the system of network snakes.

First, the *iterative solution* of the method requires both, an initialization and a stopping criterion. Different approaches are feasible to stop the processing: from a methodical point of view, the energy minimization has converged, when the movement of the contour network is zero. Practically, the stopping criterion is activated when the movement is below a specified threshold.

Second, several *parameters* control the energy functional of network snakes (18). The internal energy $E_{\text{int}}(C(s))$ is influenced by two parameters α and β to incorporate shape characteristics of the object of interest (cf. Sect. 2). In addition, the parameter κ includes modeled knowledge in the minimization process to weight the image energy $E_{\text{img}}(C(s))$ and the internal energy $E_{\text{int}}(C(s))$. The parameter γ defines the step size during the iterative minimization (18). The parameters have to be predefined properly or, alternatively, could be defined automatically with given reference contours in terms of a supervised parameter tuning.

Third, the introduction and, moreover, the exploitation of the *topology* has to be considered as the prominent challenge of this work. The concept of parametric active contours as basis of the new graph-based method requires a given topology which is assumed to be correct. Furthermore, the exploitation of a given correct topology during the energy minimization process presumes the preservation of this initial topology. This fact cannot be guaranteed in general, because close contour parts can merge or nodes with higher degrees can move around each other. These undesired effects mean that the result does not necessarily correspond to a planar graph any longer. The preservation of the correct initial topology must be ensured during the complete processing to avoid touching or overlapping contour parts and, thus, changes of the original topology, cf. Fig. 4 for a negative example. To solve this problem, a *topology-preserving energy* $E_{\text{topo}}(C(s))$ is introduced to avoid changes of topology:

$$E_{\text{topo}}\left(C\left(s\right)\right) = \frac{1}{d_{\text{topo}}\left(C\left(s\right)\right)^2}. \tag{23}$$

The parameter $d_{\text{topo}}(C(s))$ with $0 < d_{\text{topo}} < d_{\max}$ describes the distance between two neighboring contour parts. Consequently, a convergence of two contours becomes more expensive within the energy minimization process as the distance between two contours becomes smaller and, thus, practically the introduction of E_{topo} inhibits merging. The distance is not introduced as a linear force but instead as a quadratic term, because the interesting point of control arises when object contours are close to each other. In this case, a quadratic term leads to the desired stronger push-off effect. In addition, the influence of the topology-preserving energy to the

Fig. 4 Synthetic example without the topology-preserving energy: initialization (*blue*), optimization steps (*white*) and result (*red*)

Fig. 5 Synthetic example including the topology-preserving energy: initialization (*blue*), optimization steps (*white*) and result (*red*)

total energy functional can be restricted by an upper limit $d_{\max}$, because neighboring contours will only influence each other within a specific spacing. In the vicinity of nodes with a degree $\rho(C) > 2$ representing the junctions of a contour network, the topology-preserving energy is not considered due to the intended intersection. Hence, the positioning of neighboring contour parts within the network is monitored and controlled during the processing. In Fig. 5, the same initialization is used as in Fig. 4. The topology-preserving energy $E_{\text{topo}}(C(s))$ enables the exploitation of topology during the energy minimization and yields a correct result.

4 Results and analysis

4.1 Goals of the analysis

The main goal of the analysis is to highlight the benefits and limitations of the proposed new method of network snakes. The focus is on issues resulting from the newly introduced topology to the concept of parametric active contours. The interesting point to be analyzed is the question of which potential from active contours can be tapped when the topology is exploited during the optimization of the energy functional. Taking up the goals of this article, the following issues are analyzed and evaluated.

Initialization Network snakes are based on the concept of parametric active contours. Hence, an initialization close to the true object boundary is required to enable the local optimization process. The aim of the analysis is to formulate rules, how the term close initialization can be defined and which requirements have to be considered. Furthermore, dependencies between the shape characteristics of the object of interest, the image characteristics and the initialization are content of the investigations.

Topology The introduction of topology to parametric active contours is the main innovation of this work. The question is to which extent network snakes can improve results or allow for coarser initializations of the contour. In addition, the relation of the topology to the image data representing the object of interest is a prominent part of the examinations to point out the contribution of the topology to overcome disturbances or less concise and fragmented image features.

Generality and transferability Another goal of the work is the generality and transferability of the developed mathematical model. Thus, the applicability of the new model is tested with different synthetic and real application scenarios.

4.2 Synthetic examples

In Figs. 6–14, synthetic examples are given to demonstrate and analyze the relation between initialization, topology and image data. The arbitrary synthetic examples composed of homogeneous adjacent regions were chosen such that any disturbing influencing factors can be ignored. Naturally, the synthetic examples represent networks themselves by the borderlines of the adjacent regions, too. The derived image energy is based on the distance potential force computed from the edge map of the synthetic examples.

The starting point of the optimization of the energy functional $E(C(s))$ of network snakes is a given *initial contour network*. In general, an initial contour network will move to the closest image features, which can be expected regarding the mathematical definition of the image energy $E_{\text{img}}(C(s))$. In Fig. 6, the middle part of the right vertical contour is initialized beyond a critical position, i.e. closer to the wrong object contour, which would cause a wrong final result optimizing this contour part *separately* using traditional parametric active contours. In contrast, network snakes consider the *complete network* simultaneously during the optimization of the energy functional and, in particular, exploit the connectivity of the individual contour parts. Consequently, the adjacent and correctly initialized contour parts guide the middle part step by step to the correct result. The internal energy $E_{\text{int}}(C(s))$ has a dominant weight compared to the image energy $E_{\text{img}}(C(s))$ of the total energy functional to control the network snake while exploiting the given initial topology. In Fig. 7, an increased critical initialization with several wrong initial contour parts within the complete network is chosen. Both wrongly initialized contour parts

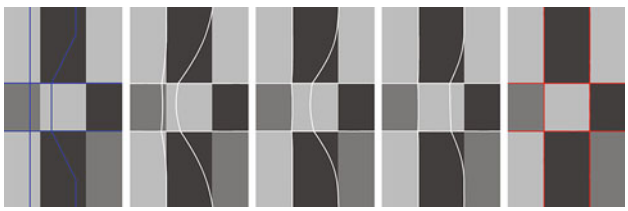

Fig. 6 Initialization of network snakes exploiting the topology during the optimization: initialization (*blue*), optimization steps (*white*) and result (*red*)

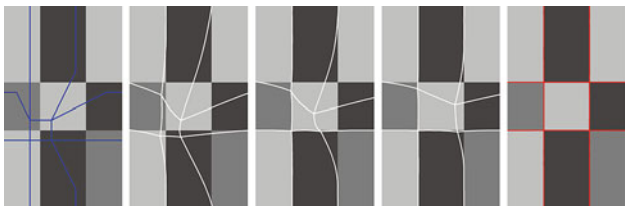

Fig. 7 Critical initialization of network snakes exploiting the topology during the optimization: initialization (*blue*), optimization steps (*white*) and result (*red*)

in the middle of the horizontal and vertical contour, respectively, move as part of the network step by step to the correct result. In general, contour parts farther away from the object boundaries are more influenced by the internal energy compared to the image energy, which is why the topology has such a large impact to the optimization process. Thus, the introduction and exploitation of the topology to the concept of parametric active contours enables weaker initialization requirements compared to the traditional concept.

Concluding the initialization requirements, the following rule can be established: The length of the contour parts, discretized by the number of nodes $C_0, \ldots, C_n$, with shorter distances to the true object boundary has to be *larger* than of those contour parts with shorter distances to wrong contour parts

$$\sum_{i=C_0}^{C_n} \left(d_{\text{correct}} < d_{\text{wrong}}\right) > \sum_{i=C_0}^{C_n} \left(d_{\text{correct}} > d_{\text{wrong}}\right). \tag{24}$$

The parameter d_{correct} is defined as the difference between the initial contour and the correct object boundary $d_{\text{correct}} = |C_{\text{init}} - O_{\text{correct}}|$, and the parameter d_{wrong} is defined as the difference between the initial contour and an arbitrary wrong object boundary $d_{\text{wrong}} = |C_{\text{init}} - O_{\text{wrong}}|$ for the coordinates x and y, respectively. The rule in (24) incorporates the conditions of equal magnitudes of the image energy and a larger weight of the internal energy $E_{\text{int}}(C(s))$ compared to the image energy $E_{\text{img}}(C(s))$, i.e. the parameter κ is defined as $0 < \kappa < 1$. It has to be noted, that the established rule above has a very theoretical background. Using real data and real application scenarios, the estimation of the required conditions could be difficult. Thus, the left part of (24) must be guaranteed to be large enough to compensate in particular disturbing image characteristics and the uncertainty of how close the contour network is initialized to the true object boundary.

A main benefit of the proposed new method of network snakes is the *exploitation* of the *topology* during the energy minimization process. However, the requirement is a given topology which is assumed to be correct. In addition, the preservation of the topology during the optimization process has to be ensured within the complete processing to avoid touching or overlapping contour parts, which change the initial correct topology. The second prerequisite has been solved with the introduction of the topology-preserving energy $E_{\text{topo}}(C(s))$ to the energy functional as defined in Sect. 3.2. Since the prerequisite assuming a given correct topology cannot always be guaranteed, the *influence* of a *wrong topology* is analyzed next. In particular, the impact of a partly wrong topology to the result of the given adjacent correct parts of the graph is investigated. In Figs. 8 and 9 one and two contour parts, respectively, are added to the initial network. The influence of the additional wrong contour part

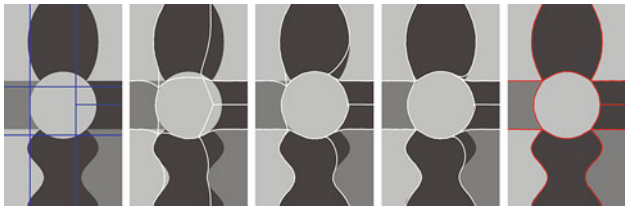

Fig. 8 Optimization of network snakes exploiting a wrong topology with one surplus contour part: initialization (*blue*), optimization steps (*white*) and result (*red*)

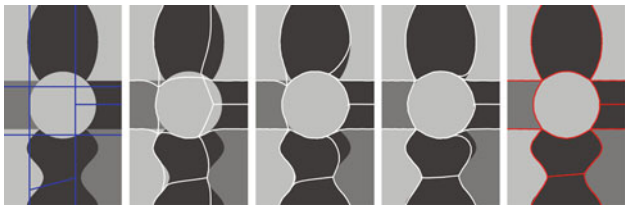

Fig. 9 Optimization of network snakes exploiting a wrong topology with two surplus contour parts: initialization (*blue*), optimization steps (*white*) and result (*red*)

to the adjacent correct parts of the network is relatively insignificant, even though the shape model of some contours is split. The final result delineates the object borders correctly, and the surplus contour parts move to the minimum without the presence of a related object border. Consequently, the introduction of surplus contour parts to a correct initial topology does not influence the adjacent correct contour parts of the network in the final result.

In Figs. 10 and 11, one and two contour parts, respectively, are *eliminated* leading to an incomplete representation of the

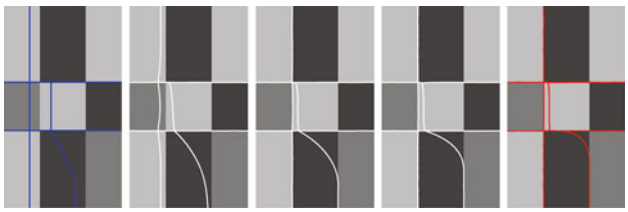

Fig. 10 Optimization of network snakes exploiting a wrong topology with one missing contour part: initialization (*blue*), optimization steps (*white*) and result (*red*)

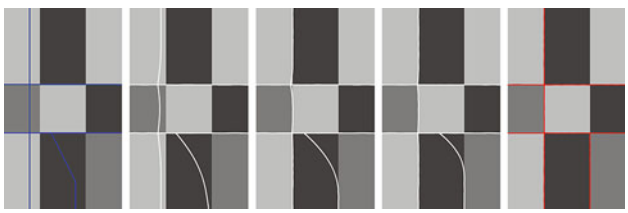

Fig. 11 Optimization of network snakes exploiting a wrong topology with two adjacent missing contour parts: initialization (*blue*), optimization steps (*white*) and result (*red*)

topology of the objects of interest. Starting the optimization of the contour network it is apparent that the missing contour part results in a missing delineation of the respective object boundary. Compared to the optimization exploiting the correct topology, the adjacent contour part in the middle of the vertical contour is not able to reach the true object boundary. The topology-preserving energy $E_{\text{topo}}(C(s))$ prevents a merging with the left contour part, but the final result of the network comprises not only one missing but in addition two wrong contour parts (Fig. 10). The exploitation of the topology enables the delineation of wrongly initialized contour parts due to the connectivity to adjacent correctly initialized contour parts concerning the initialization requirements. But, as already mentioned above, the length of the contour parts with shorter distances to the true object boundary has to be larger than that of the contour parts with shorter distances to a wrong boundary. In contrast to the investigations depicted in Fig. 10, the contour part shown in Fig. 11 at the bottom moves to the correct object boundary. The underlying reason for this fact is the same as the one for the failure described just before: in this case, the length of the contour pieces with shorter distances to the true object boundary is larger, which is why the adjacent missing contour part has no adverse effect. In conclusion, missing or surplus contour parts in the network lead to missing or surplus delineations of the respective object boundaries caused by the fixed topology. An initial wrong topology caused by missing boundaries can result in wrongly delineated adjacent contour parts, if the adjacent contours are incorrectly initialized. A concept to involve a correction of the topology simultaneously with the exploitation of the topology during the energy minimization is needed to resolve this problem, but is beyond the scope of this paper.

All analysis carried out in this section so far is based on *ideal object representations* within the image to define a clear framework for the investigations focusing only on the respective contents of interest. However, the assumption of given ideal object boundaries cannot be ensured, in particular, when using real application scenarios. Thus, the effect of the *topology* to deal with *poor* or *fragmented object representations* is investigated next, see Figs. 12, 13 and 14. The corresponding images are generated by randomly cutting holes out of the object representation, in Fig. 14 Gaussian noise is added accessorily. The fragmented or blurred edge image is the input for the distance map. Contour parts, which are directly influenced by object boundaries and, thus, are represented with attracting forces in the image energy, move faster to the object boundaries compared to those parts, where the holes cause a neutral image energy. In all examples the concerned parts in the contour network can be delineated successfully as a result of the integrated internal energy $E_{\text{int}}(C(s))$ and the topology within the energy functional. The added Gaussian noise in Fig. 14 blurs the precise object

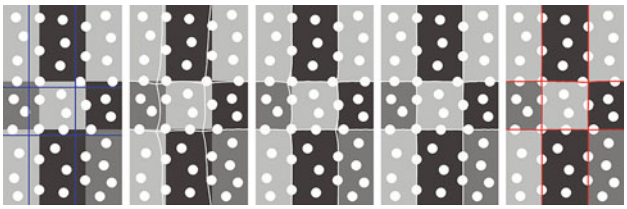

Fig. 12 Impact of the topology to slightly fragmented object representations in the image, white blobs represent holes: initialization (*blue*), optimization steps (*light gray*) and result (*red*)

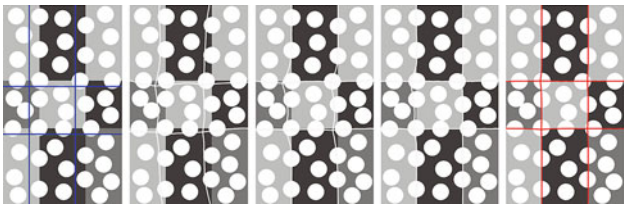

Fig. 13 Impact of the topology to strongly fragmented object representations in the imagery, white blobs represent holes: initialization (*blue*), optimization steps (*light gray*) and result (*red*)

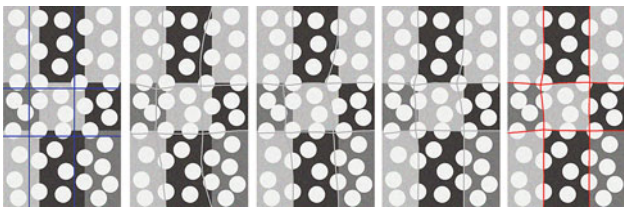

Fig. 14 Impact of the topology to strongly fragmented object representations in the imagery with added Gaussian noise, white blobs represent holes: initialization (*blue*), optimization steps (*light gray*) and result (*red*)

borders: this worsening becomes critically when the object is only represented by very small object features, e.g. very small edge features between close holes. In general, the established statements in this section involve a balanced parameter setting to enable the preservation of the shape model during the complete optimization process. Here, the parameters are defined with $\alpha = 0.1$, $\beta = 2$, $\gamma = 6$ and $\kappa = 0.9$. The point of a balanced parameter setting is important, because the intended exploitation of the topology is related to the initialization requirements, the parameter control and the iteration behavior.

The shown synthetic examples in Figs. 12, 13 and 14 point out the benefit and robustness of network snakes based on parametric active contours due to the direct exploitation of the topology together with the image energy and the internal energy. The topology is the crucial factor to deal with fragmented and blurry object representations in imagery. In addition, only locally available image information at

networks or adjacent object borders has a purposive effect to the correct result, if region-based image information within the enclosed network segments is not useable due to heterogeneous object classes. This fact points out the advantage of the proposed method compared to geometric active contours.

4.3 Real examples

Regarding the defined goals at the beginning of this section, two points have not been investigated so far: the analysis of the *generality and transferability* of the proposed new method of network snakes, and, the contribution of the *topology* concerning its impact to overcome disturbances or less concise object feature represented in real imagery. These goals are analyzed with three real application scenarios: the delineation of *field boundaries* from remotely sensed images, the refinement of *road networks* using airborne SAR images and the delineation of *adjacent biological cells* in microscopic cell images. The detection of field boundaries is an important task for the geo-sciences and the agricultural sector, for example for the derivation of field-based risks of soil loss, precision farming or the monitoring of subsidies. The geometric refinement of road networks to improve GIS-databases is the topic of many current investigations to improve the basic data for traffic navigation and planning. The detection of cells and their derived properties regarding shape, size and intensity distribution is an increasingly important task in bio-medical research such as pharmaceutical drug discovery. All examples are chosen to demonstrate the transferability to different applications and, moreover, the examples are well-suited to point out the impact of the proposed new method of network snakes.

In Fig. 15, a typical example of a pan-sharpened IKONOS CIR-image with a ground resolution of 1.0 m is shown, displayed is a part of 1,000 × 1,000 pixels. The delineation of field boundaries is started with a preliminary segmentation realized as an automatic system with a combination of a region- and edge-based approach: a multi-channel region growing is carried out using all available channels in a coarser resolution, because at that point the geometric accuracy is not essential. Neighboring pixels are aggregated into one and the same region, if the difference in color does not exceed a predefined threshold. In addition, extracted edges, evaluated concerning their length and straightness, are introduced into the region growing process to restrict expansion beyond potential field boundaries. The derived initial contour network consists of 120 contour parts represented by 1,850 nodes (Fig. 15, top). The end points of the contour network with a degree $\rho(C) = 1$ at the image borders are chained there and are allowed to move only along the borderline. The image energy is derived from the standard deviation of the intensity channel of the CIR-image within a quadratic

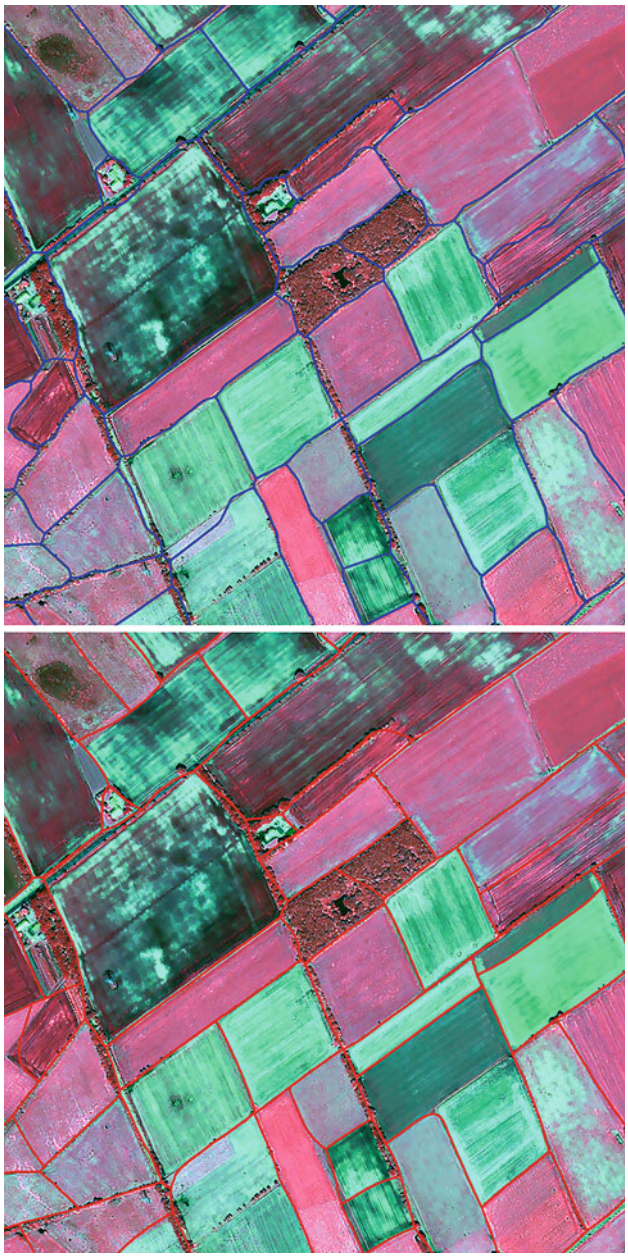

Fig. 15 Delineation of field boundaries from remotely sensed imagery. *Top* initialization of network snakes using the initial segmentation (*blue*). *Bottom* final result of the optimization using network snakes (*red*)

mask, because high values typically belong to field boundaries. Since the objects to be delineated are rather straight, the parameter β is set to a large value compared to α, i.e. $\alpha = 0.1$, $\beta = 30$, $\gamma = 6$ and $\kappa = 0.9$. In the presented examples in this section, the parameters are constant for every node to ease the comparison of the results. Of course, a more flexible parameter setting is possible to introduce prior shape-knowledge about specific contour parts, for example different parameters can be selected at or near corners.

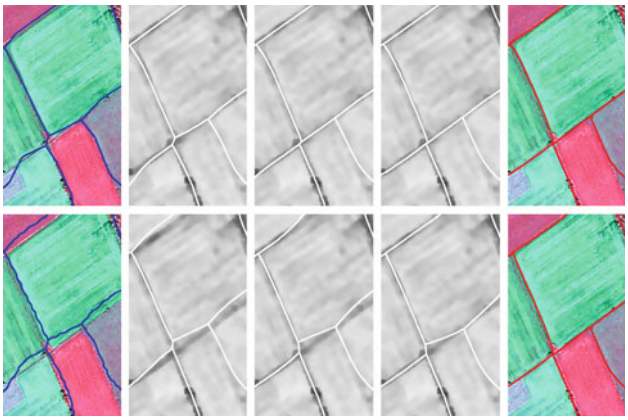

Fig. 16 *Top series* detail of the utilization of network snakes shown in Fig. 15 using the correct initial segmentation. *Bottom series* upwards shifted initialization of network snakes. *Both series* initialization (*blue*), optimization steps superimposed to the image energy (*white*) and final result (*red*)

The optimization applying network snakes aims to improve the geometric accuracy of the field boundaries exploiting the image energy, the internal energy and the topology in a simultaneous optimization of the contour network (Fig. 15, bottom). The initial segmentation is compared to the reference data within a buffer of 10 pixels obtaining a completeness of 79%, a correctness of 83% and the geometric accuracy as expressed in the planimetric root mean square value is 4.9 pixel equivalent to 4.9 m. The segmentation reflects a typical result concerning the completeness and correctness; only a few initial boundaries are missing. In addition, the result after applying the network snakes is compared to the reference data within a buffer of 10 pixels: the completeness increases to 83%, the correctness to 87% and the geometric accuracy improves about 36% to 3.6 pixel or 3.6 m. The refinement is rather good, because the geometric accuracy achieves a quality which is provided by the information contained in the image representing the field boundaries. In particular, the heterogeneous structures within the fields cannot support region-based image information and, additionally, the field boundaries are mostly represented only with blurry features. Thus, the newly introduced and the joint graph-based optimization enable the good delineation even though the object representation is poor. The improvement of the completeness and correctness represents an enhancement of the field boundaries, which are contained in the buffer of 10 m and, thus, are usable for this specific application compared to the initial segmentation.

The automatic segmentation used as *real* initialization to start the optimization process (Figs. 15, 16, top series) is exemplarily *shifted upwards* to vary the initialization conditions (Fig. 16, bottom series). Now, the completeness of 47% and the correctness of 48% of the shifted initialization are considerably worsened compared to the correct initialization. But, the optimization using network snakes improves both quality measures to nearly identical values compared to the results obtained with the original initial segmentation, i.e. the completeness improves to 73% and the correctness to 78%. In addition, the geometric accuracy improves about 55% to 3.8 pixel or 3.8 m using the shifted initialization, which is more or less the same compared to the geometric accuracy using the correct initialization. The results demonstrate that a moderate shift of the initialization can be compensated using network snakes.

In Fig. 17, an airborne SAR image with a ground resolution of 1.0 m is shown, displayed is a part of $900 \times 1{,}000$ pixels. The geometric refinement of the road network is initialized with road data taken from a GIS database (Fig. 17, left). The contour network consists of 27 contour parts represented by 1,200 nodes. Again, the end points of the contour network at the image borders are chained there allowing movement only along the borderline. The image energy is derived from the Laplace of Gaussian (LoG) operator of the SAR image, because the result represents roads in a discriminable way compared to the local background. Since the objects to be delineated are rather straight, comparable to the delineation of field boundaries, the parameters are set identically with $\alpha = 0.1$, $\beta = 30$, $\gamma = 6$ and $\kappa = 0.9$. The initial GIS database road network is compared to reference data within a buffer of 25 pixels yielding a completeness of 92% and a correctness of 100%. The buffer of 25 pixels guarantees the consideration of all database objects, the reduced completeness is caused by few missing roads in the database (lower right part of Fig. 17). However, the focus is on the geometric accuracy as expressed in the planimetric root mean square value which is only 9.6 pixel equivalent to 9.6 m. The result after applying the network snakes is compared to the reference data within the same buffer: obviously, the completeness of 92% and the correctness of 100% are kept constant, but the geometric accuracy increases to 2.6 pixel or 2.6 m. This improvement is very good, in particular considering the complex properties of the SAR image caused by the typical speckle-effect, layover and shadowing. The benefit of network snakes exploiting the topology during the graph-based optimization together with the image energy and the internal energy is evidently. In addition, only the local image information at the network has a purposive effect to the correct result, because the region-based image information within the enclosed road network segments is not useable due to the different object classes (settlement, fields, grassland) (Fig. 18). This fact points out the advantage of the proposed method compared to the latest research of multiple adjacent geometric active contours (cf. Sect. 2).

In Fig. 19, typical multi-channel fluorescence labeling are shown with a size of 200×200 pixels: cell nuclei image (left) and microscopic cell image (middle). Each cell

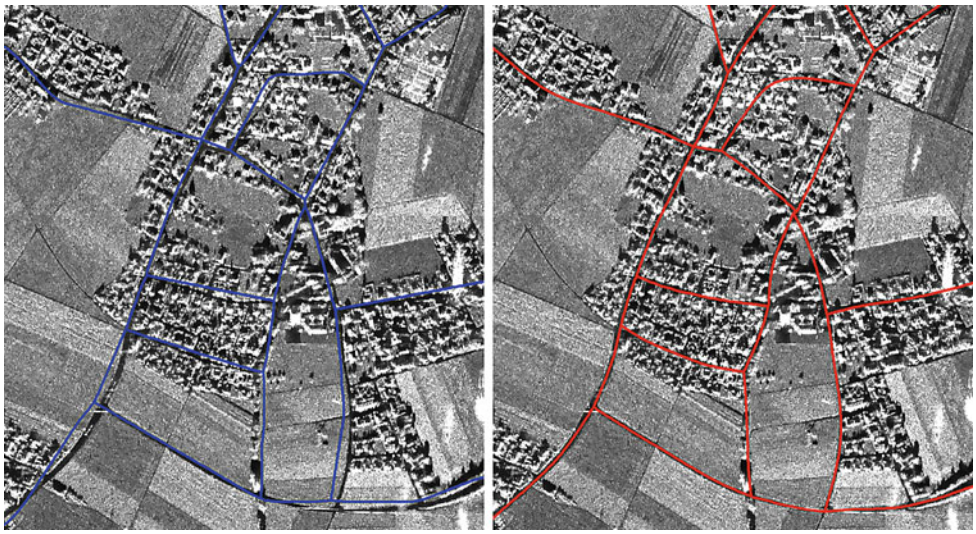

Fig. 17 Delineation of a road network from airborne SAR image. *Left* initialization of network snakes using the road database (*blue*). *Right* final result of the optimization using network snakes (*red*)

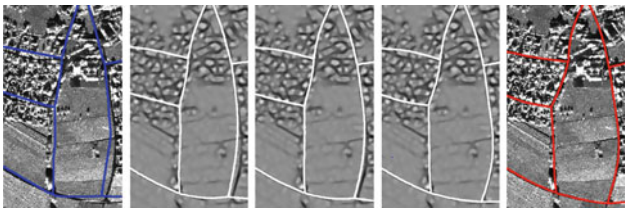

Fig. 18 Detail of the utilization of network snakes shown in Fig. 17: initialization (*blue*), optimization steps superimposed to the image energy (*white*) and final result (*red*)

nucleus is located within the associated cell membrane, which allows to take this information as seed point to derive the topology delineating the boundaries of adjacent cells. The segmentation of the cell nuclei within the first channel leads to a contour network with 48 contour parts represented by 1,500 nodes (Fig. 19, left). Obviously, the detection of all cell nuclei leads to a correct topology. The initial segmentation process is compared to manually derived reference data in a 10 pixel wide buffer, 10 pixels are equivalent to approximately 1.5 µm. Thus, the requirement of a minimum accuracy for the usability of cells is reached considering the provided resolution and noise within the image. All cell nuclei are detected correctly, which leads to quality measures of 100% for both, completeness and correctness. The geometric accuracy as expressed in the root mean square value is 3.1 pixel. This strategy is well-known in detecting and tracking cells, because the machine-dependent artifacts like noise and typical object characteristics like homogeneous areas in the intensity distribution at cell boundaries cause major difficulties using only one image channel. The network snakes approach is used to optimize and improve the accuracy using the second channel representing the cytoplasm (Fig. 19, middle, right). Since the objects to be delineated have a specific range of curvature, the parameter β is set to a large value compared to α, but is not set to such a large value compared to the delineation of mostly straight field boundaries or roads, i.e. $\alpha = 0.1$, $\beta = 10$, $\gamma = 6$ and $\kappa = 0.9$. The final result is compared to the reference data: obviously, the completeness and correctness are kept constant at 100%, but the geometric accuracy increases to 2.9 pixel. The improvement of the complete network is only moderate, because the optimization works well in the center of the example, but works poorly at the borders of the image. This fact is confirmed regarding only the quality measures in the center of the example excluding the border area: the initial geometric accuracy with 3.0 pixel is similar compared to the complete initialization, but after the optimization using network snakes the accuracy increases to 2.2 pixel. The different improvement of the cells concerning the whole example and the center area is caused by the exploitation and impact of the topology. In particular, noisy image data and weak object representations in the image energy point out the benefit of the introduced topology. Moreover, the results demonstrate the general advantage of network snakes compared to geometric active contours and area-based segmentation methods, because the poor object representation and the difficult discrimination of the objects require the utilization of local image information combined with global topologically knowledge.

In Fig. 20, a detail of Fig. 19 is shown (top series). In contrast, the part of the example shown in Fig. 20 (bottom series) does not include the topology- preserving energy $E_{\text{topo}}(C(s))$ defined in Sect. 3.2. Thus, the two neighboring nodes, which are close to each other located on the right side, move around each other and change the correct initial topology leading to a wrong result. The example demonstrates the impact of the utilization and preservation of the topology. The other depicted

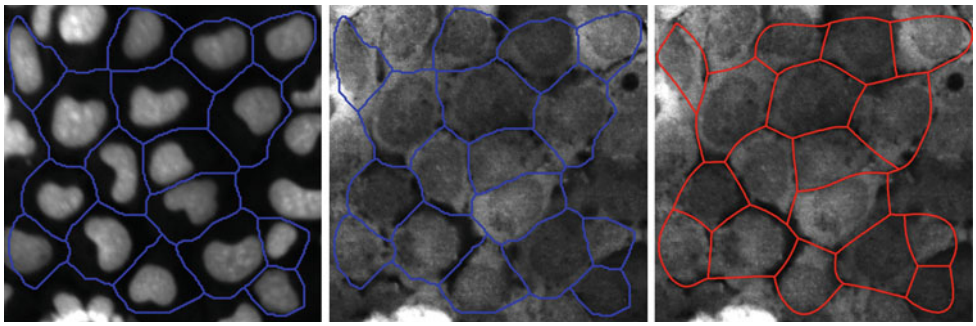

Fig. 19 Delineation of biological cells. *Left* cell nuclei with derived initialization (*blue*). *Center* initialization superimposed to the microscopic cell imagery (*blue*). *Right* final result of the delineation of cells using network snakes (*red*)

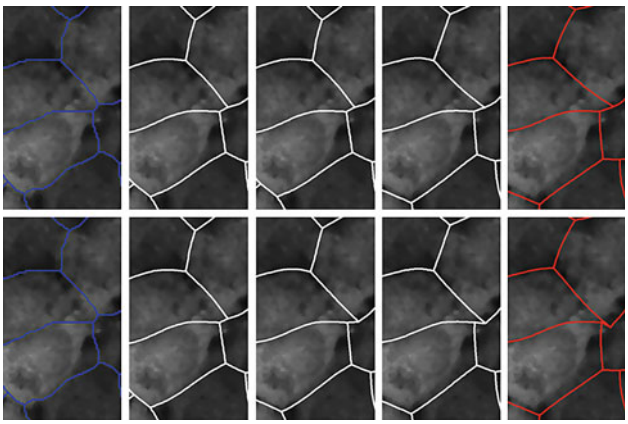

Fig. 20 *Top series* detail of the utilization of network snakes shown in Fig. 19 incorporating the topology-preserving energy. *Bottom series* detail of the utilization of network snakes without the incorporation of the topology-preserving energy. *Both series* initialization (*blue*), optimization steps superimposed to the image energy (*white*) and final result (*red*)

contour parts of the network move to the correct boundaries of the cells, even though the object representation within the image energy is not very distinct.

5 Conclusions

The main goal of the paper was the introduction and overall investigation of the general framework of network snakes, which enables the delineation of arbitrary graphs representing the geometric position of networks and boundaries between adjacent objects. The presented method solves this task with the introduction of a graph-based model based on the concept of parametric active contours. In addition, the role of the required initialization, the generality and transferability of the approach was investigated with a systematic analysis of synthetic and real images in order to point out the usefulness of the new method for a large variety of different applications. The main impact of network snakes is the combination of the image energy representing the objects in the real world, the internal energy incorporating the shape characteristics, and the topology representing the structure of the scene in a common comprehensive energy functional.

The analysis of the results shows, that adjacent objects without any available homogeneous object characteristics within the segments and, moreover, objects represented directly by networks independently of object and purposive image information of enclosed network segments, can be well delineated. Thus, the introduction and exploitation of the topology is a very prominent factor to deal with fragmented and blurry object representations in imagery. Hence, the well-known active contour models as an important method in computer vision are enhanced and can be employed for a new class of objects.

Two main points are of special interest for possible future research: The first point concerns the given *rigid topology* in conjunction with the dependence on the quality of the *initialization.* The question is whether a potential change in the topology can be introduced into the proposed mathematical model and whether the dependence on the initial position of the network can be reduced in this way. The underlying concept of parametric active contours includes an explicit representation of contours in their parametric form during the deformation process resulting in rigid topology. This fact involves three issues: first, an initialization needs to be provided; second, the initial topology is assumed to be correct; and, third, the given topology must be preserved in terms of a planar graph during the optimization process. The third point has been fulfilled with the incorporation of the topology-preserving energy $E_{\text{topo}}(C(s))$. The first and second point constitute important constraints regarding the given initialization and topology. The local optimization involves a dependence on the given initialization. The exploitation of the topology reduces the role of the initial quality as shown regarding the synthetic examples. Nevertheless, the proposed method depends on initializations, thus requiring a preprocessing or segmentation step prior to the optimization. For the presented three real examples, the initialization is provided automatically using different preprocessing steps: automatic initial segmentation for the field boundary delineation, data from a GIS database for the road network refinement, and

automatic detection of cell nuclei for the delineation of adjacent biological cells. However, a common automatic preprocessing method for providing initial values for different applications is not given in this paper. A further crucial point is the issue of whether the exploitation of the rigid topology can be combined with the detection of topology errors and their elimination in one optimization process. The development of strategies and approaches to introduce the possibility to change the topology in conjunction with their exploitation is a sophisticated task for future research.

The second interesting point for possible further investigation is the question of whether an *internal evaluation* of the contour network can provide quality measures for the obtained results. The question of internal evaluation is related to the problem of rigid topology discussed above. A statement concerning the quality of a contour part during the optimization of the network can provide evidence to delete a contour part, thus changing the topology. Yet, decisions in this context could be deceptive: for example, the utilization of the image information to provide a new assessment criterion regarding a contour part could lead to a wrong decision. Active contour models have the advantage compared to other methods of combining the image energy with internal energy terms and, thus, delineating a contour correctly even though the image information is non-purposive. The introduction of the topology improves this characteristic because network snakes enable a larger independence of the image information exploiting the topology. Consequently, the utilization of the image information during the optimization to derive quality measures of the contour parts of the network is difficult. In addition, an internal evaluation requires redundant information which causes a modification of the proposed method of network snakes to derive that independent information, which up to now has not been considered. The internal evaluation of network snakes to provide quality measures and to give evidence to change the topology is thus another challenging task for further research with the aim of developing strategies to improve the general methodology of network snakes.

Acknowledgments The authors wish to thank Evotec Technologies providing the medical image data. The IKONOS images are provided by the EC-MARS Program—distributed by the European Space Imaging, EUSI, 2004.

References

1. Blake, A., Isard, M.: Active Contours. Springer, Berlin (1998)
2. Bresson, X., Esedoglu, S., Vandergheynst, P., Thiran, J.P., Osher, S.: Fast Global Minimization of the Active Contour/Snake Model. J. Math. Imaging Vis. **28**(2), 151–167 (2007)
3. Butenuth, M.: Segmentation of imagery using network snakes. Photogrammetrie Fernerkundung Geoinformation 1/2007, pp. 7–16 (2007)
4. Butenuth, M., Heipke, C.: Network snakes-supported extraction of field boundaries from imagery. In: Kropatsch, W., Sablatnig, R., Hanbury, A. (eds.) Pattern Recognition, Lecture Notes in Computer Science, vol. 3663, pp. 417–424. Springer, Berlin (2005)
5. Caselles, V., Catté, F., Coll, T., Dibos, F.: A geometric model for active contours in image processing. Numer. Math. **66**(1), 1–31 (1993)
6. Chan, T.F., Vese, L.A.: Active contours without edges. IEEE Trans. Image Process. **10**(2), 266–277 (2001)
7. Cohen, L.D., Cohen, I.: Finite element methods for active contour models and balloons for 2D and 3D images. IEEE Trans. Pattern Anal. Mach. Intell. **15**(11), 1131–1147 (1993)
8. Delagnes, P., Benois, J., Barba, D.: Active contours approach to object tracking in image sequences with complex background. Pattern Recognit. Lett. **16**(2), 171–178 (1995)
9. Delingette, H., Montagnat, J.: Shape and topology constraints on parametric active contours. Comput. Vis. Image Underst. **83**(2), 140–171 (2001)
10. Dickinson, S.J., Jasiobedzki, P., Olofsson, G., Christensen, H.I.: Qualitative tracking of 3-D objects using active contour networks. In: Proceedings of Computer Vision and Pattern Recognition, pp. 812–817 (1994)
11. Fua, P.: Parametric models are versatile: the case of model based optimization. In: International Archives of Photogrammetry and Remote Sensing III/2, pp. 828–833 (1995)
12. Fua, P., Grün, A., Haihong, L. : Optimization-based approaches to feature extraction from aerial images. In: Dermanis, A., Grün, A., Sanso, F. (eds.) Geomatic Methods for the Analysis of Data in the Earth Sciences, pp. 190–228. Springer, Berlin (1999)
13. Grün, A., Li, H.: Semi-automatic linear feature extraction by dynamic programming and LSB-snakes. Photogramm. Eng. Remote Sens. **63**(8), 985–995 (1997)
14. Han, X., Xu, C., Prince, J.L.: A topology preserving level set method for geometric deformable models. IEEE Trans. Pattern Anal. Mach. Intell. **25**(6), 755–768 (2003)
15. Jasiobedzki, P.: Adaptive adjacency graphs. In: Vemuri, B.C. (ed.) Geometric Methods in Computer Vision II, pp. 294–303 (1993)
16. Kanizsa, G.: Subjective Contours. Sci. Am. **234**(4), 48–52 (1976)
17. Kass, M., Witkin, A., Terzpopoulos, D.: Snakes: active contour models. Int. J. Comput. Vis. **1**(4), 321–331 (1988)
18. Lachaud, J., Montanvert, A.: Deformable meshes with automated topology changes for coarse-to-fine three-dimensional surface extraction. Med. Image Anal. **3**(2), 187–207 (1999)
19. Laptev, I., Mayer, H., Lindeberg, T., Steger, A., Baumgartner, A.: Automatic extraction of roads from aerial images based on scale space and snakes. Mach. Vis. Appl. **12**(1), 23–31 (2000)
20. Leitner, F., Cinquin, P.: Complex topology 3-D objects segmentation. In: Larson, R.M., Nasr, H.N. (eds.) Model-Based Vision Development and Tools. SPIE 1609, pp. 16–26 (1992)
21. Leroy, B., Herlin, I.L., Cohen, L.D.: Multi-resolution algorithms for active contour models. In: Proceedings of International Conference on Analysis and Optimization of Systems, pp. 58–65 (1996)
22. Malladi, R.: Geometric Methods in Bio-Medical Image Processing. Springer, Berlin (2002)
23. Malladi, R., Sethian, J.A., Vemuri, B.C.: Shape modeling with front propagation: a level set approach. IEEE Trans. Pattern Anal. Mach. Intell. **17**(2), 158–175 (1995)
24. McInerney, T., Terzopoulos, D.: Deformable models in medical image analysis: a survey. Med. Image Anal. **1**(2), 91–108 (1996)
25. McInerney, T., Terzopoulos, D.: Topologically adaptable snakes. In: Proceedings of International Conference on Computer Vision, pp. 840–845 (1995)
26. Merriman, B., Bence, J.K., Osher, S.J.: Motion of multiple junctions: a level set approach. J. Comput. Phys. **112**(2), 334–363 (1994)

27. Osher, S., Paragios, N.: Geometric Level Set Methods in Imaging, Vision, and Graphics. Springer, Berlin (2003)
28. Paragios, N., Deriche, R.: Geodesic active contours and level sets for the detection and tracking of moving objects. IEEE Trans. Pattern Anal. Mach. Intell. **22**(3), 266–280 (2000)
29. Paragios, N., Deriche, R.: Geodesic active regions: a new framework to deal with frame partition problems in computer vision. J. Vis. Commun. Image Represent. **13**(1), 249–268 (2002)
30. Peteri, R., Celle, J., Ranchin, T.: Detection and extraction of road networks from high resolution satellite images. In: Proceedings of International Conference on Image Processing, pp. 301–304 (2003)
31. Ray, N., Acton, S.T., Altes, T., De Lange, E.E., Brookeman, J.: Merging parametric active contours within homogeneous image regions for MRI-based lung segmentation. IEEE Trans. Med. Imaging **22**(2), 189–199 (2003)
32. Singh, A., Goldgof, D.B., Terzopoulos, D.: Deformable Models in Medical Image Analysis. IEEE Computer Society Press, Los Alamitos (1998)
33. Smith, K.A., Solis, F.J., Chopp, D.L.: A projection method for motion of triple junctions by level sets. Interfaces Free Bound. **4**(3), 263–276 (2002)
34. Sundaramoorthi, G., Yezzi, A.: Global regularizing flows with topology preservation for active contours and polygons. IEEE Trans. Image Process. **16**(3), 803–812 (2007)
35. Suri, J.S., Setarehdan, S.K., Singh, S.: Advanced Algorithmic Approaches to Medical Image Segmentation: State-of-the-Art Applications in Cardiology, Neurology, Mammography and Pathology. Springer, Berlin (2002)
36. Unal, G., Yezzi, A., Krim, H.: Information-theoretic active polygons for unsupervised texture segmentation. Int. J. Comput. Vis. **62**(3), 199–220 (2005)
37. Vese, L.A., Chan, T.F.: A multiphase level set framework for image segmentation using the Mumford and Shah Model. Int. J. Comput. Vis. **50**(3), 271–293 (2002)
38. Williams, D.J., Shah, M.: A fast algorithm for active contours and curvature estimation. CVGIP: Image Underst. **55**(1), 14–26 (1992)
39. Wolf, B., Heipke, C.: Automatic extraction and delineation of single trees from remote sensing data. Mach. Vis. Appl. **18**(5), 317–330 (2007)
40. Xu, C., Prince, J.L.: Gradient vector flow: a new external force for snakes. In: Proceedings of IEEE Conference on Computer Vision and Pattern Recognition, pp. 66–71 (1997)
41. Xu, C., Prince, J.L.: Snakes, shapes, and gradient vector flow. IEEE Trans. Image Process. **7**(3), 359–369 (1998)
42. Yezzi, A., Tsai, A., Willsky, A.: A statistical approach to snakes for bimodal and trimodal imagery. In: Proceedings of International Conference on Computer Vision, pp. 898–903 (1999)
43. Zhang, B., Zimmer, C., Olivo-Marin, J.: Tracking fluorescent cells with coupled geometric active contours. In: Proceedings of International Symposium on Biomedical Imaging: Nano to Macro, pp. 476–479 (2004)
44. Zhao, H., Chan, T., Merriman, B., Osher, S.: A variational level set approach to multiphase motion. J. Comput. Phys. **127**(1), 179–195 (1996)
45. Zhu, S.C., Lee, T.S., Yuille, A.L.: Region competition: unifying snakes, region growing, and Bayes/MDL for multiband image segmentation. In: Proceedings of International Conference on Computer Vision, pp. 416–425 (1995)
46. Zhu, S.C., Yuille, A.L.: Region competition: unifying snakes, region growing, and Bayes/MDL for multiband image segmentation. IEEE Trans. Pattern Anal. Mach. Intell. **18**(9), 884–900 (1996)
47. Zimmer, C., Olivo-Marin, J.: Coupled parametric active contours. IEEE Trans. Pattern Anal. Mach. Intell. **27**(11), 1838–1842 (2005)

Author Biographies

Matthias Butenuth graduated with a Dipl.-Ing. degree in 2002 in Geodesy and Geoinformatics and received the Dr.-Ing. degree in 2008, both from the Leibniz Universität Hannover, Germany. Since 2007 he holds the position of a research assistant at the Remote Sensing Technology Department of Technische Universität München, Germany, since 2008 he is additionally the deputy head of the Remote Sensing Technology Department. His research interests comprise computer vision, pattern recognition and image analysis, in particular for the interpretation of high-resolution imagery and image sequences as well as industrial real-time applications. The second research field is remote sensing regarding satellite-based Earth observation, multi-sensor fusion with GIS-data and 4D-SAR. He is the author and coauthor of about 40 international papers, most of them peer-reviewed. In 2008, he was presented the Otto von Gruber Award, the most prestigious award for young scientists offered by the International Society for Photogrammetry and Remote Sensing (ISPRS), recognizing a particularly important scientific publication. Currently, he serves as secretary of the ISPRS working group III/5 "Image Sequence Analysis".

Christian Heipke studied Geodetic Sciences and Surveying at the universities of Hannover, Sydney, and Munich. He graduated from the Technical University Munich in 1986 and subsequently joined the Industrieanlagen-Betriebsgesellschaft (IABG), Ottobrunn as a Research Scientist. In 1990, he became Research Fellow at the Chair for Photogrammetry and Remote Sensing, Technical University Munich. In the same year, he received a Ph.D. degree (Dr.-Ing.) and in 1994 the venia legendi (Dr.-Ing. habil.), both from TU Munich. Form 1991 to 1994, he led the research group 'Digital Photogrammetry' at the same institution. Throughout 1995 he was a visiting professor for photogrammetry at Ohio State University, Columbus, OH. He returned to TU Munich at the beginning of 1996, where he headed the research group 'Image matching and object extraction'. He was awarded another visiting professorship at Ecole Polytechnique Fédérale de Lausanne, Switzerland in spring 1998. In October 1998, he was appointed Head of the Institute of Photogrammetry and GeoInformation, Leibniz Universität Hannover, where he currently leads a group of about 25 researchers, most of them funded through grants from national and international science organisations and from industry. His professional interests comprise all aspects of digital photogrammetry and remote sensing, image understanding and their connection to GIS. His two areas of special expertise are (a) automatic sensor orientation and (b) object extraction from images. He is the recipient of the Otto von

Gruber Award 1992, the most prestigious award for young scientists offered by the International Society for Photogrammetry and Remote Sensing (ISPRS). He has more than 60 refereed publications in scientific journals to his name. From 2004 to 2009, he served as chair of the ISPRS working group IV/3 "Automated geo-spatial data acquisition and mapping" and as vice president of EuroSDR (European Spatial Data Research, formerly known as OEEPE).